LOS Signal Identification for Passive Multi-Target Localization in Multipath Environments

Yifan Liang, and Hongbin Li, *Fellow, IEEE*

***Abstract*—This paper examines line-of-sight (LOS) path identification for passive multi-target localization in multipath environments. We consider a system comprising multiple spatially distributed sensors, each transmitting a distinct waveform and using the echoes to measure the LOS and non-LOS (NLOS) delays (i.e., ranges) of the targets in the surveillance area. For simplicity, we assume a 2-dimensional localization scenario, where each range measurement defines a circle, and measurements from different sensors create intersection points on the plane. The problem is to identify intersections that are created by LOS paths. To solve the problem, we classify the intersections into $N(N-1)/2$ types, where N denotes the number of sensors. Then, an efficient clustering algorithm is proposed to efficiently identify the LOS intersections based on the type and other related attributes. Numerical results are presented to demonstrate the performance of the proposed technique in comparison with several peer methods.**

***Index Terms*—Multi-target localization, passive targets, multipath propagation, line-of-sight (LOS) identification**

I. Introduction

Target localization is a crucial requirement in diverse applications encompassing navigation, augmented reality, industrial automation, and the Internet of Things [1]–[6]. Among various localization approaches, delay-based methods offer superior localization precision when paired with wideband probing signals [7]–[15]. There are two types of localization problems. In *active* localization, the target (e.g., a mobile wireless device) transmits a distinct signal received by sensors [16], whereas in *passive* localization, the target, which is RF-silent, is illuminated by an external transmitter, and the target echo is utilized for localization. Passive localization poses more significant challenges, especially in a multi-path environment with multiple targets (see Fig. 1) [17]–[19]. In particular, with the same illuminator, all targets reflect the same waveform. As such, a non-line-of-sight (NLOS) echo of one target can be confused as a line-of-sight (LOS) echo of another target. The problem is generally less challenging in active cases, where different targets emit distinct waveforms, which can be exploited for differentiation.

Target localization relies on LOS paths to find targets. If some prior knowledge is available, such as when the statistics of the excess delay of the NLOS path are known [16], [20] or multiple NLOS observations are geometrically constrained with one another [21], [22], LOS and NLOS measurements can be properly combined for target localization. Without such prior knowledge, NLOS paths will cause non-negative bias in location estimates [16], [20], [23]. Various LOS detection methods have been investigated for active and passive localization problems [20], including hypothesis testing [24]–[26] and nonparametric techniques [27]–[32]. Most of these methods, however, were developed for active single-target localization in multipath environments, and they are in general ineffective for passive multipath multi-target localization.

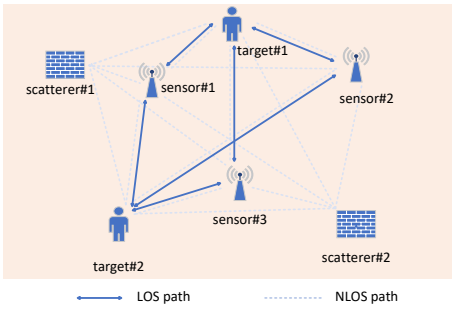

Fig. 1. A multi-sensor localization system with multiple passive targets and scatterers (non-target objects) in a multipath environment.

We consider herein LOS identification for a delay-based passive localization system consisting of multiple distributed sensors. Each sensor measures the LOS and NLOS ranges of the targets, thus creating numerous intersections in the surveillance area. We propose a *type-based* clustering algorithm to identify intersections that are created by LOS paths. Following LOS identification, the multi-target localization problem reduces to multiple single-target problems which can be solved by conventional localization methods.

II. Problem Formulation

Consider a multi-sensor system comprising N sensors at $\mathbf{a}_n \in \mathbb{R}^2, n = 1,\ldots,N$, which is employed to locate K targets at unknown locations $\mathbf{p}_k \in \mathbb{R}^2, k = 1,\ldots,K$. The environment also consists of L non-target scatterers at locations $\mathbf{s}_l \in \mathbb{R}^2, l = 1,\ldots,L$. Each sensor probes the environment by sending a unique waveform and measures the time delays of target/scatterer echoes by using a matched filter [16]. The delay measurements translate to LOS and NLOS range observations that are described by

$$\begin{aligned} r_{n,k} &= \|\mathbf{p}_k - \mathbf{a}_n\| + \epsilon_{n,k}, \\ y_{n,k,l} &= \|\mathbf{p}_k - \mathbf{a}_n\| + \|\mathbf{p}_k - \mathbf{s}_l\| + \|\mathbf{s}_l - \mathbf{a}_n\| + \epsilon_{n,k,l}, \\ n \in \{1,\ldots,N\}, &\quad k \in \{1,\ldots,K\}, \quad l \in \{1,\ldots,L\} \end{aligned} \tag{1}$$

This work was supported by the National Science Foundation under grant ECCS-1923739, ECCS-2212940, and CCF-2316865.

Corresponding author: Hongbin Li.

Yifan Liang and Hongbin Li are with the Department of Electrical and Computer Engineering, Stevens Institute of Technology, Hoboken, NJ 07030 USA (e-mail: yliang33@stevens.edu; hli@stevens.edu).

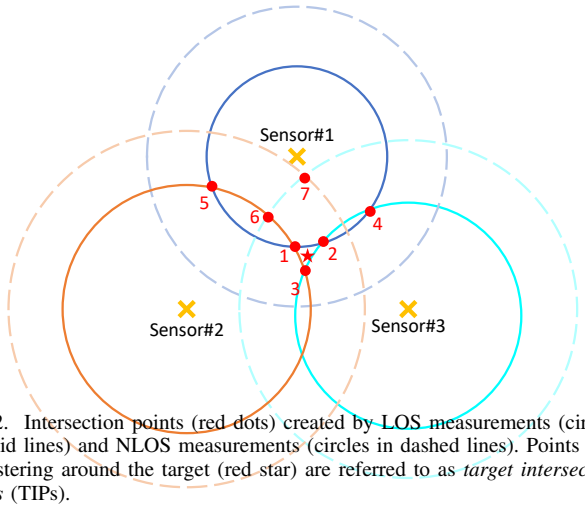

Fig. 2. Intersection points (red dots) created by LOS measurements (circles in solid lines) and NLOS measurements (circles in dashed lines). Points 1 to 3 clustering around the target (red star) are referred to as *target intersection points* (TIPs).

where ϵ denotes the range measurement noise with zero mean and variance σ^2. The multi-sensor system cannot distinguish between LOS measurements $r_{n,k}$ and NLOS measurements $y_{n,k,l}$, nor can it identify which target each measurement is related to. The problem of interest is to develop an algorithm for identifying $r_{n,k}$ of each target by exploiting some inherent geometric structure of the data.

III. Proposed Approach

A. Main Idea

Each delay-based range measurement defines a circle centered at the corresponding sensor's location, and such circles produce many intersection points. Consider the ideal case in the absence of noise. The N circles defined by $r_{n,k}, n = 1,\ldots,N$, referred to as the *LOS circles* associated with target k, intersect at the target location $\mathbf{p}_k$, whereas the *NLOS circles* defined by $y_{n,k,l}$ do not.

In scenarios with measurement noise, LOS circles no longer intersect at $\mathbf{p}_k$. Instead, as shown in Fig. 2, they create some intersections close to $\mathbf{p}_k$, e.g., points 1, 2, and 3. Such intersections are called *target intersection points* (TIPs). In contrast, points 4 and 5 are *non-target intersection points* (NTIPs) that are isolated from one another, although they are intersected by LOS circles. LOS-NLOS intersections (e.g., point 6) and NLOS-NLOS intersections (e.g., point 7) are also NTIPs. The LOS identification problem is therefore transformed to finding TIPs among the numerous intersections on the plane.

The presence of noise makes the problem even harder by causing two LOS circles to cease to intersect, leading to the disappearance of a TIP, a phenomenon referred to as *point loss*. To circumvent this, if two circles do not intersect, we implement a recovery procedure where the radius of each circle is increased/decreased by a small amount κ to create expanded/shrunk circles, where κ typically falls between $\sigma/2$ and 2σ, where σ denotes the standard deviation of the range measurements. If the expanded or shrunk circles intersect at two points, they are nearly tangent to each other since κ is small. Therefore, the average of the coordinates of the two points is included in the existing set of intersections for LOS identification. Through simulations, we found the above approach effectively mitigates the negative effect of point loss.

B. Type-Based Clustering Algorithm (TCA)

Given all intersection points, TCA is an efficient clustering algorithm that produces K clusters of points, denoted by $\mathcal{V}_k, k = 1,\ldots,K$, one for each target. Each cluster $\mathcal{V}_k$, referred to as a *TIP set*, is composed of the TIPs associated with target k. TCA is a type-based algorithm, which classifies all intersection points into a total of $N(N-1)/2$ *types*. Each type corresponds to the pair of sensors producing the intersection. TCA utilizes the following concepts.

Definition 3.1 (Type Set): The points belonging to the same type are referred to as a *type set*, expressed as $\mathcal{T}_{n_1,n_2} \triangleq \{x \in \mathbb{R}^2 | x = \mathcal{C}_{n_1} \cap \mathcal{C}_{n_2}, n_1 \neq n_2\}$, where $\mathcal{C}_n$ denotes the set of circles centered at the n-th sensor.

Definition 3.2 (Spread): The *spread* of a point set $\mathcal{U}$, denoted by $s(\mathcal{U})$, is defined as the sum of the standard deviation of the x- and, respectively, y-coordinates of all points in $\mathcal{U}$.

Definition 3.3 (Parent Circles): Each point in a point set $\mathcal{U}$ is produced by two intersecting circles. *Parent circles* of $\mathcal{U}$, denoted by $\mathcal{P}(\mathcal{U})$, consist of the set of all circles that are involved in producing the points in $\mathcal{U}$ by intersection.

A TIP set has several properties that can be used for identification. Most of them are straightforward to show.

Property 3.1 (TIP Set Number): The total number of TIP sets is K, denoted by $\mathcal{V}_k, k = 1,\ldots,K$, one for each target.

Property 3.2 (Type Uniqueness): Each point in $\mathcal{V}_k$ has a unique type and $|\mathcal{V}_k| = N(N-1)/2$, i.e., $\mathcal{V}_k$ has all types of points.

Property 3.3 (Size of Parent Circle Set): $|\mathcal{P}(\mathcal{V}_k)| = N$. This is because each TIP set is created by intersections of N LOS circles respectively centered at each sensor.

Property 3.4 (Non-overlapping): $\mathcal{V}_{k_1} \cap \mathcal{V}_{k_2} = \emptyset, \forall k_1 \neq k_2$, i.e., different TIP sets are non-overlapping.

Every point on the plane is either a TIP or NTIP. TCA exploits the above concepts/properties to screen all points in an efficient way. The algorithm consists of a two-stage search process followed by a final screening.

1) Stage-1 Search: Stage 1 focuses on $(N-1)$ intersection types $\mathcal{T}_{1,2},\ldots,\mathcal{T}_{1,N}$, starting from $\mathcal{T}_{1,2}$. Note that sensor labeling is random, i.e., they can be labeled in any order. Hence, $\mathcal{T}_{1,2}$ can be any type set for initialization. We form the initial candidate TIP sets, each containing a unique point from $\mathcal{T}_{1,2}$, and these candidate sets are represented by $\mathcal{U}_j^1, j = 1,\ldots,J_1$, where $J_1 = |\mathcal{T}_{1,2}|$. These candidate sets, each containing a single point, are designated *size*-1 *candidate sets* as denoted by the superscript $(\cdot)^1$. For example, point 1 in Fig. 2 forms a candidate set, which is a TIP. Point 5 also forms a candidate set, which is a NTIP. Candidate sets containing NTIPs are later eliminated by checking against points of other types.

We proceed to $\mathcal{T}_{1,3}$ and check if any of its points can be included in the existing candidate sets. For an existing candidate set, say $\mathcal{U}_j^1$, a point x in $\mathcal{T}_{1,3}$ can be included in $\mathcal{U}_j^1$ if $|\mathcal{P}(\mathcal{U}_j^1 \cup x)| = 3$, i.e., the size of the parent set of $\{\mathcal{U}_j^1 \cup x\}$ is 3, which means that that point x must share 1 circle with the circles associated with $\mathcal{U}_j^1$. This can be seen in Fig. 2, where $\mathcal{U}_1^1 = \{\text{point } 1\}$ can be expanded with point 2 to form a new candidate set, $\mathcal{U}_1^2 = \{\text{point } 1, \text{point } 2\}$ since point 2 adds only a new circle (the cyan solid circle) to $\mathcal{P}(\mathcal{U}_1^1)$.

Only 1 point can be included in an existing candidate set for expansion. If multiple points meet the criterion, different new candidate sets need to be formed. For example, point 4 also meets the parent circle criterion for $\mathcal{U}_1^1$, and they can be combined into a new size-2 candidate set $\mathcal{U}_2^2 = \{\text{point 1, point 4}\}$. Note that a point may be selected by multiple different candidate sets, as long as it meets the parent circle criterion. Those size-1 candidate sets that fail to integrate with a $\mathcal{T}_{1,3}$ point based on the parent circle criterion are eliminated. Furthermore, to reduce the number of candidates, we can eliminate those sets comprising points that are far away from each other, i.e., those with a spread measure exceeding a threshold γ.

The next step is to go through the points in $\mathcal{T}_{1,4}$, and expand size-2 candidate sets into size-3 candidate sets. The process is repeated until we have finished with $\mathcal{T}_{1,N}$, which results in a series of size-$(N-1)$ candidate sets $\mathcal{U}_j^{N-1}, j = 1, \ldots, J_{N-1}$.

The above search process ensures each candidate set $\mathcal{U}_j^{N-1}$ contains $(N-1)$ points of distinct types (i.e., sensor pairs) that are created by the intersections of N parent circles centered at the N sensors. Consider again the 3-sensor example in Fig. 2. $\mathcal{U}_1^2 = \{\text{point 1, point 2}\}$, which contains $N-1=2$ points of distinct types, i.e., $\mathcal{T}_{1,2}$ and $\mathcal{T}_{1,3}$ respectively.

2) Stage-2 Search: The purpose of Stage-2 search is to examine the points in the remaining Types $\mathcal{T}_{n_1,n_2}, n_1 > 1, n_2 = 3, \ldots, N$, one type at a time, by following similar steps used in Stage-1 search with one exception. Specifically, recall in Stage 1, a point x is included in an existing candidate set $\mathcal{U}_j^m, m = 1, \ldots, N-2$, if and if only x *increases the size of the parent set of* $\mathcal{U}_j^m$ *by 1*. In Stage 2, a point x can be included in an existing candidate TIP set $\mathcal{U}_j^m, m = N-1, N, \ldots$, if and only if x *retains the size of the parent set of* $\mathcal{U}_j^m$*, which is N*. This, again, can be illustrated by the 3-sensor example. Stage-1 search has produced a number of size-2 candidate sets, including $\mathcal{U}_1^2$={point 1, point 2}. To expand $\mathcal{U}_1^2$ to a size-3 candidate TIP set, we can add a point from Type $\mathcal{T}_{2,3}$. For example, point 3 can be included to form $\mathcal{U}_1^3$= {point 1, point 2, point 3}, which keeps the parent set size unchanged, i.e., $|\mathcal{U}_1^3| = |\mathcal{U}_1^2| = N = 3$. In contrast, point 6, which is also a $\mathcal{T}_{2,3}$ point, cannot be used to expand the candidate set since it would increase the parent set size to 4, whereas a real TIP set should be produced by N and only N parent circles.

3) Final Screening: At the end of Stage-2 search, we have a few size-$N(N-1)/2$ candidate sets $\mathcal{U}_j, j = 1, \ldots, J_{N(N-1)/2}$, where the superscript is dropped for notational simplicity and $J_{N(N-1)/2}$ denotes the number of the final candidate TIP sets, which depends on the threshold γ. These candidate TIP sets are guaranteed to satisfy Properties 3.2 and 3.3. The final screening process is to determine the final TIP sets from the candidate sets by imposing Property 3.4 along with the fact that the points within a TIP set are close to one another with a small spread.

A summary of TCA is presented in Algorithm 1, which is non-iterative and guaranteed to produce K TIP set estimates $\mathcal{U}_1^*, \ldots, \mathcal{U}_K^*$. Note that $\mathcal{P}(\mathcal{U}_k^*)$, i.e., the parent circles of $\mathcal{U}_k^*$, comprises N circles, each centered at a unique sensor. The radii of these circles, denoted by $\hat{r}_{n,k}, n = 1, \ldots, N$, represent estimates of the LOS ranges in (1).

[1]The superscript $N(N-1)/2$ is next dropped for simplicity.

Algorithm 1: Type-based Clustering Algorithm (TCA)

Input: $\mathcal{T}_{n_1,n_2}, n_1 = 1, \ldots, N-1, n_2 = 2, \ldots, N$, spread threshold γ, target number K

Output: K TIP set estimates $\mathcal{U}_k^*, k = 1, \ldots, K$

Initialization:
  $\mathcal{U}_j^1 = \{x_j | x_j \in \mathcal{T}_{1,2}\}, j = 1, \ldots, J_1 \triangleq |\mathcal{T}_{1,2}|$; $t = 2$
Stage-1 Search:
while $t < N-1$ **do**
  Set $v = 1$
  for *each* x *in* $\mathcal{T}_{1,t+1}$ **do**
    for $j = 1, \ldots, J_{t-1}$ **do**
      if $s(\{\mathcal{U}_j^{t-1} \cup x\}) \le \gamma$ **and** $|\mathcal{P}(\{\mathcal{U}_j^{t-1} \cup x\})| = t+1$ **then**
        $\mathcal{U}_v^t = \{\mathcal{U}_j^{t-1} \cup x\}$
        $v = v + 1$
  $J_t = v$
  $t = t + 1$
Stage-2 Search:
Rename $\mathcal{T}_{n_1,n_2}, n_1 \ge 2, n_2 \ge 3$ as a single-indexed set sequence $\mathcal{T}_t', t = 1, \ldots, (N-1)(N-2)/2$
Initialization: $t = 1$, $m = N-1$
while $t \le (N-1)(N-2)/2$ **do**
  Set $v = 1$
  for *each* x *in* $\mathcal{T}_t'$ **do**
    for $j = 1, \ldots, J_m$ **do**
      if $s(\{\mathcal{U}_j^m \cup x\}) \le \gamma$ **and** $|\mathcal{P}(\{\mathcal{U}_j^m \cup x\})| = N$ **then**
        $\mathcal{U}_v^{m+1} = \{\mathcal{U}_j^m \cup x\}$
        $v = v + 1$
  $J_{s+1} = v$
  $t = t + 1$
  $m = m + 1$
Final Screening:
Let $\mathcal{S} = \{\mathcal{U}_j^{N(N-1)/2}, j = 1, \ldots, J_{N(N-1)/2}\}$[1]
for $i, j = 1, \ldots, J_{N(N-1)/2}, i \ne j$ **do**
  if $\mathcal{U}_j \cap \mathcal{U}_i \ne \emptyset$ **and** $s(\mathcal{U}_j) \ge s(\mathcal{U}_i)$ **then**
    Remove $\mathcal{U}_j$ from $\mathcal{S}$
Reorder $\mathcal{S}$ in increasing spread. The first K sets are selected as TIP set estimates, denoted by $\mathcal{U}_k^*$, $k = 1, \ldots, K$.

C. Target Localization

Once the LOS measurements corresponding to the K targets are respectively identified, the multi-target localization problem is converted into several single-target localization problems, which can be solved by several existing methods, such as the *range-based least squares* (R-LS) estimator and the squared-range-based least squares (SR-LS) estimator [33].

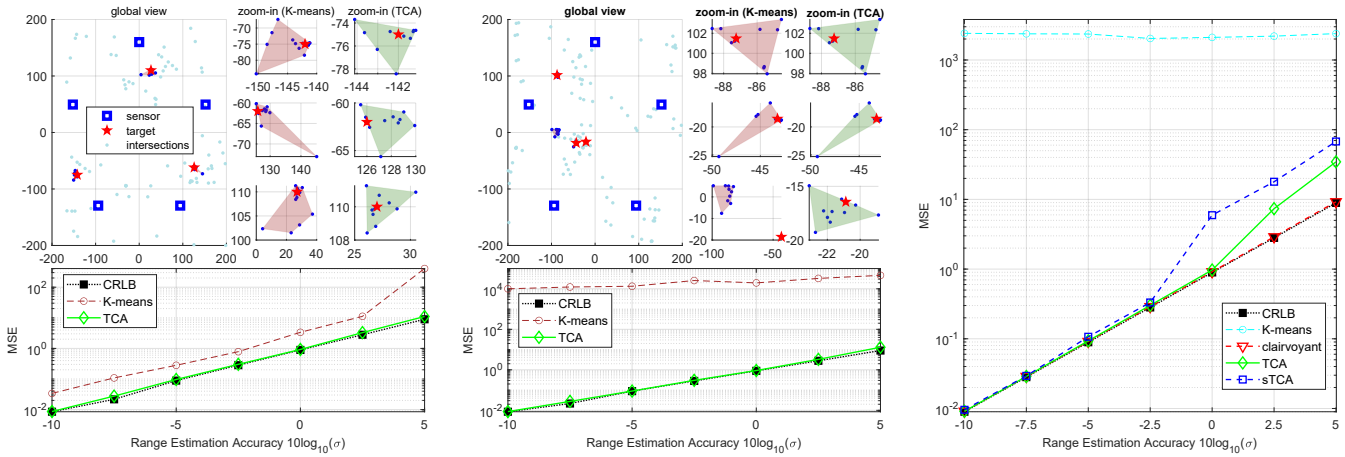

(a) (b) (c)

Fig. 3. (a) Results in a scenario with *well-separated* and *fixed* target locations. Upper left: a global view of sensors/targets/intersections with $\sigma = 1$. Upper right: estimates of the target intersection point (TIP) sets obtained by K-mean and TCA with $\sigma = 1$, where each colored area represents the convex hull of the points within an estimated TIP set. Lower: MSE when target locations are fixed with varying σ. (b) Result with another fixed-target location scenario, where K-mean fails to identify all TIP sets. (c) MSE with *randomly varying target locations*.

In this paper, we use R-LS for target localization:

$$\text{(R-LS)}: \quad \min_{\mathbf{p}_k} \sum_{n=1}^{N} \left(\hat{r}_{n,k} - \|\mathbf{p}_k - \mathbf{a}_n\|\right)^2 . \tag{2}$$

Clearly, the localization performance of (2) is critically dependent on the accuracy of the LOS identification rendered by TCA. The relation is examined numerically next.

IV. Simulation Results

In this section, experimental results are presented to show the performance of different methods. We compare **TCA** and a simplified version, denoted by **sTCA**, which is obtained by skipping the stage-2 search of TCA. Another method included in comparison is the **K-means** clustering algorithm, which divides all points on the plane into multiple clusters and the generated clusters that contain more than $N(N-1)/2$ points are selected as candidate sets. Similar to the screening process of TCA, K clusters among the candidate sets with the smallest spread are chosen and their centroids are regarded as the location estimates of K targets. Additionally, a **clairvoyant** method is included which locates the target by (2) with precise knowledge of the LOS measurements. Finally, all methods are compared with the Cramer-Rao lower bound (**CRLB**) [16].

The surveillance area is a 400×400 square area centered at $(0, 0)$ on the plane. The system has $N = 5$ sensors uniformly distributed on a circle centered at $(0, 0)$ with a radius 160. The environment contains $L = 4$ scatterers randomly located on the border of the square, where the locations of the sensors and scatterers are fixed during simulations, and $K = 3$ targets, whose locations vary randomly from one trial to another. The measurement noise is independent and identically distributed Gaussian random variable with zero mean and variance σ^2. For TCA and sTCA, we set $\kappa = 2\sigma$ for point recovery (cf. Section III-A). The mean squared error (MSE) is obtained with 600 independent simulations and further averaged over all targets.

The performance of K-means is sensitive to the target locations. Fig.3(a) depicts an example where the targets are *well separated* and *fixed* in simulations. The target clusters found by both K-means and TCA are relatively close to the true target locations. The MSE of K-means is about 3 at $\sigma = 1$, whereas the MSE of TCA is about 1. However, in another case with fixed target locations depicted in Fig.3(b), K-means is unable to locate one of the two closed-spaced targets. As a result, its MSE averaged over all targets is orders of magnitude worse than that of TCA.

Fig. 3(c) depicts the MSE of all considered methods, when the target locations are randomly changing within the surveillance area from one trail to another. It is seen that TCA is nearly identical to the clairvoyant method and close to the CRLB when range estimates are relatively accurate, i.e., $10\log_{10}(\sigma) \leq 0$. TCA also outperforms sTCA, especially with less accurate range estimates. On the other hand, the MSE of K-means is significantly higher than all other methods, since it sometimes produces very poor target location estimates in some scenarios. In contrast, TCA works well in both cases. As shown in Fig.3(c), TCA gives a reliable performance with all noise levels. Moreover, Stage 2 of TCA helps improve the robustness and accuracy of the algorithm.

V. Conclusion

We examined a multi-static delay-based sensing system for passive multi-target localization in multipath environments. Based on the geometric characteristics of range measurements, we proposed a TCA algorithm for LOS path identification. The algorithm takes into account the point loss phenomenon and consists of two stages of searching and a final screening process. TCA assumes that each sensor has LOS measurements of all targets. A future direction is to consider the case of missing LOS measurements as some sensors might be blocked from some targets in practice.

REFERENCES

[1] A. Yassin, Y. Nasser, M. Awad, A. Al-Dubai, R. Liu, C. Yuen, R. Raulefs, and E. Aboutanios, "Recent advances in indoor localization: A survey on theoretical approaches and applications," *IEEE Communications Surveys & Tutorials*, vol. 19, no. 2, pp. 1327–1346, 2016.

[2] R. C. Shit, S. Sharma, D. Puthal, and A. Y. Zomaya, "Location of things (LoT): A review and taxonomy of sensors localization in iot infrastructure," *IEEE Communications Surveys & Tutorials*, vol. 20, no. 3, pp. 2028–2061, 2018.

[3] F. Zafari, A. Gkelias, and K. K. Leung, "A survey of indoor localization systems and technologies," *IEEE Communications Surveys & Tutorials*, vol. 21, no. 3, pp. 2568–2599, 2019.

[4] Y. Zheng, M. Sheng, J. Liu, and J. Li, "Exploiting AoA estimation accuracy for indoor localization: A weighted AoA-based approach," *IEEE Wireless Communications Letters*, vol. 8, no. 1, pp. 65–68, 2019.

[5] K. Wen, C. K. Seow, and S. Y. Tan, "An indoor localization and tracking system using successive weighted RSS projection," *IEEE Antennas and Wireless Propagation Letters*, vol. 19, no. 9, pp. 1620–1624, 2020.

[6] N. Sahu, L. Wu, P. Babu, B. S. MR, and B. Ottersten, "Optimal sensor placement for source localization: A unified ADMM approach," *IEEE Transactions on Vehicular Technology*, vol. 71, no. 4, pp. 4359–4372, 2022.

[7] Y. T. Chan and K. Ho, "A simple and efficient estimator for hyperbolic location," *IEEE transactions on signal processing*, vol. 42, no. 8, pp. 1905–1915, 1994.

[8] K. W. Cheung, H.-C. So, W.-K. Ma, and Y. T. Chan, "Least squares algorithms for time-of-arrival-based mobile location," *IEEE transactions on signal processing*, vol. 52, no. 4, pp. 1121–1130, 2004.

[9] Y. Sun, K. Ho, and Q. Wan, "Solution and analysis of TDOA localization of a near or distant source in closed form," *IEEE Transactions on Signal Processing*, vol. 67, no. 2, pp. 320–335, 2018.

[10] G. Wang, W. Zhu, and N. Ansari, "Robust TDOA-based localization for IoT via joint source position and NLOS error estimation," *IEEE Internet of Things Journal*, vol. 6, no. 5, pp. 8529–8541, 2019.

[11] A. Chugunov, N. Petukhov, and R. Kulikov, "TOA positioning algorithm for TDOA system architecture," in *2020 International Russian Automation Conference (RusAutoCon)*, 2020, pp. 871–876.

[12] T. Wang, H. Xiong, H. Ding, and L. Zheng, "TDOA-based joint synchronization and localization algorithm for asynchronous wireless sensor networks," *IEEE transactions on communications*, vol. 68, no. 5, pp. 3107–3124, 2020.

[13] Y. Sun, K. Ho, Y. Yang, L. Zhang, and L. Chen, "Computationally attractive and statistically efficient estimator for noise resilient TOA localization," *Signal Processing*, vol. 200, p. 108663, 2022.

[14] G. Yang, Y. Yan, H. Wang, and X. Shen, "Improved robust TOA-based source localization with individual constraint of sensor location uncertainty," *Signal Processing*, vol. 196, p. 108504, 2022.

[15] M. Lin, W. Wang, and C. Liu, "Preventing hostile TOA/TDOA localization with af relay," *IEEE Communications Letters*, vol. 27, no. 4, pp. 1085–1089, 2023.

[16] S. Gezici, Z. Tian, G. Giannakis, H. Kobayashi, A. Molisch, H. Poor, and Z. Sahinoglu, "Localization via ultra-wideband radios: a look at positioning aspects for future sensor networks," *IEEE Signal Processing Magazine*, vol. 22, no. 4, pp. 70–84, 2005.

[17] F. Wang, H. Li, X. Zhang, and B. Himed, "Signal parameter estimation for passive bistatic radar with waveform correlation exploitation," *IEEE Transactions on Aerospace and Electronic Systems*, vol. 54, no. 3, pp. 1135–1150, 2017.

[18] F. Zhang, Y. Sun, J. Zou, D. Zhang, and Q. Wan, "Closed-form localization method for moving target in passive multistatic radar network," *IEEE Sensors Journal*, vol. 20, no. 2, pp. 980–990, 2019.

[19] X. Zhang, F. Wang, H. Li, and B. Himed, "Maximum likelihood and IRLS based moving source localization with distributed sensors," *IEEE Transactions on Aerospace and Electronic Systems*, vol. 57, no. 1, pp. 448–461, 2020.

[20] S. Aditya, A. F. Molisch, and H. M. Behairy, "A survey on the impact of multipath on wideband time-of-arrival based localization," *Proceedings of the IEEE*, vol. 106, no. 7, pp. 1183–1203, 2018.

[21] Y. Shen and M. Z. Win, "On the use of multipath geometry for wideband cooperative localization," in *GLOBECOM 2009-2009 IEEE Global Telecommunications Conference*. IEEE, 2009, pp. 1–6.

[22] K. Witrisal, P. Meissner, E. Leitinger, Y. Shen, C. Gustafson, F. Tufvesson, K. Haneda, D. Dardari, A. F. Molisch, A. Conti *et al.*, "High-accuracy localization for assisted living: 5g systems will turn multipath channels from foe to friend," *IEEE Signal Processing Magazine*, vol. 33, no. 2, pp. 59–70, 2016.

[23] Y. Wang, K. Gu, Y. Wu, W. Dai, and Y. Shen, "NLOS effect mitigation via spatial geometry exploitation in cooperative localization," *IEEE Transactions on Wireless Communications*, vol. 19, no. 9, pp. 6037–6049, 2020.

[24] İ. Güvenç, C.-C. Chong, F. Watanabe, and H. Inamura, "NLOS identification and weighted least-squares localization for UWB systems using multipath channel statistics," *EURASIP Journal on Advances in Signal Processing*, vol. 2008, pp. 1–14, 2007.

[25] A. Conti, M. Guerra, D. Dardari, N. Decarli, and M. Z. Win, "Network experimentation for cooperative localization," *IEEE Journal on Selected Areas in Communications*, vol. 30, no. 2, pp. 467–475, 2012.

[26] S. Bartoletti, A. Giorgetti, M. Z. Win, and A. Conti, "Blind selection of representative observations for sensor radar networks," *IEEE Transactions on Vehicular Technology*, vol. 64, no. 4, pp. 1388–1400, 2015.

[27] M. Heidari, F. O. Akgul, N. A. Alsindi, and K. Pahlavan, "Neural network assisted identification of the absence of direct path in indoor localization," in *IEEE GLOBECOM 2007-IEEE Global Telecommunications Conference*. IEEE, 2007, pp. 387–392.

[28] N. Decarli, D. Dardari, S. Gezici, and A. A. D'Amico, "LOS/NLOS detection for UWB signals: A comparative study using experimental data," in *IEEE 5th International Symposium on Wireless Pervasive Computing 2010*. IEEE, 2010, pp. 169–173.

[29] S. Marano, W. M. Gifford, H. Wymeersch, and M. Z. Win, "NLOS identification and mitigation for localization based on UWB experimental data," *IEEE Journal on selected areas in communications*, vol. 28, no. 7, pp. 1026–1035, 2010.

[30] H. Wymeersch, S. Maranò, W. M. Gifford, and M. Z. Win, "A machine learning approach to ranging error mitigation for UWB localization," *IEEE transactions on communications*, vol. 60, no. 6, pp. 1719–1728, 2012.

[31] J. Shen and A. F. Molisch, "Estimating multiple target locations in multipath environments," *IEEE transactions on wireless communications*, vol. 13, no. 8, pp. 4547–4559, 2014.

[32] S. Aditya, A. F. Molisch, N. Rabeah, and H. M. Behairy, "Localization of multiple targets with identical radar signatures in multipath environments with correlated blocking," *IEEE Transactions on Wireless Communications*, vol. 17, no. 1, pp. 606–618, 2017.

[33] A. Beck, P. Stoica, and J. Li, "Exact and approximate solutions of source localization problems," *IEEE Transactions on Signal Processing*, vol. 56, no. 5, pp. 1770–1778, 2008.